JCTC Journal of Chemical Theory and Computation

Structures and Electronic States of Permethyloligosilane Radical Ions with All-Trans Form $Si_n(CH_3)_{2n+2}^{\pm}$ ($n = 2-6$): A Density Functional Theory Study

Hiroto Tachikawa*

Division of Molecular Chemistry, Graduate School of Engineering, Hokkaido University, Sapporo 060−8628, Japan

Hiroshi Kawabata

Venture Business Laboratory, Kyoto University, Kyoto 606−8501, Japan

Received May 9, 2006

Abstract: Hybrid density functional theory (DFT) calculations have been carried out for the radical cation and anion of permethyloligosilane $Si_n(CH_3)_{2n+2}^{\pm}$ ($n = 2-6$) to elucidate the electronic structures at ground and low-lying excited states, and the results were compared with the corresponding experimental values. In particular, the assignment of electronic transition appeared at near-IR and visible regions, which is strongly correlated to hole and electron conductivity, and was carried out on the basis of time-dependent DFT calculation. The structure of oligosilane was generated at 300 K by direct PM3 molecular dynamics calculations, and then the geometry was fully optimized at the DFT(B3LYP)/6-311+G(d,p) level. It was found that the hole in the radical cation and the electron in the radical anion of oligosilane are delocalized over the Si skeleton. The proton-hyperfine coupling constants calculated were in good agreement with those obtained by an electron spin resonance experiment. It was also found that the g-anisotropy of the radical anion was significantly larger than that of the radical cation. The IR bands of radical ions were assigned on the basis of theoretical calculations.

1. Introduction

Polysilane is a one-dimensional σ-conjugated polymer composed of Si−Si single bond and organic side groups.[1,2] This polymer has recently received much attention because of its potential ability as a hole and electron transport material in organic multilayer light emitting diodes, a photoresistor in lithography, and a one-dimensional semiconductor.[3−10]

To elucidate the mechanism of the electron and hole transfer processes, experimental and theoretical works for the radical cation and anion of poly- and oligosilanes have been extensively examined. Ban et al. measured transient absorption spectra of polysilanes in organic solvents after electron beam irradiation and found that the radical ions (cation and anion) of polysilanes show a strong absorption band at the UV region.[11,12] They assigned this strong peak to an electronic transition of unpaired electrons on the Si−Si skeleton. Irie et al.[13,14] measured the transient and steady-state absorption spectra of radical ions of polysilanes with aryl groups and found both UV and near-IR bands. They assigned the near-IR band to a charge resonance band between two aryl groups. Ushida et al.[15] attributed the near-IR band to charge resonance between adjacent σ-conjugated polymer segments. However, the electronic structure of radical ions of polysilanes, especially the origin of the near-IR band, is still in controversy. The low-lying excited states

* Corresponding author fax: +81 11706-7897; e-mail: hiroto@eng.hokudai.ac.jp.

10.1021/ct600163r CCC: $37.00
Published on Web 11/09/2006

in the radical ion are strongly correlated with electron (or hole) conductivity. In particular, the near-IR band of radical ions of polysilane reflects directly the ability of conductivity.

To elucidate more detailed features for the electronic states of polysilanes, an approach to use the oligomer of polysilane has been carried out by several groups. Irie et al.[16] examined chain-length dependence on the absorption spectra of the radical anion and cation of oligosilanes. The spectra observed have two peaks in the UV and near-IR regions as well as those of polysilanes, and the maxima in both spectra shifted to longer wavelengths with increasing chain length. Kumagai et al.[17,18] investigated absorption spectra of radical ions of permethyl oligosilanes. They found that the radical ions possess UV and near-IR bands, as well as those of usual polysilanes.

The magnetic properties of the radical ions have been investigated from hyperfine-coupling constants (hfcc's) and **g**-tensor components using electron spin resonance (ESR) measurements.[17,18] The ESR spectra of the radical cation of oligo- and polysilanes give a broad symmetric single line with averaged g values ranging from 2.0070 to 2.0100, which is slightly larger than that of the free electron ($g_e = 2.0023$). On the other hand, ESR spectra of the radical anion of polysilanes give an axially symmetric line shape. The radical anion of oligosilane also gives an ESR spectrum with g values in the range 2.000−2.0040. The g anisotropy decreases with increasing chain length (n).

The hfcc's of radical ions of oligosilanes have been measured by Kumagai et al.[17,18] They observed ESR spectra of radical ions of permethyloligosilanes, $Si_n(CH_3)_{2n+2}$ where n ranges from 2 to 6. For $n = 2$, the smallest radical cation, the hfcc of the proton is measured to be 0.57 mT. The hfcc's decreased with increasing n: for example, hfcc's for $n = 4$ and 6 are 0.55 and 0.19 mT ($n = 4$) and 0.39, 0.29, and 0.11 mT ($n = 6$).

The electronic states of neutral oligosilanes have been investigated mainly by ab initio calculations.[19,20] Michl and Ottosson investigated conformers of n-$Si_6(CH_3)_{14}$ using ab initio, molecular mechanics, and additive increment methods.[19a] It was found that all-transoid is the most stable conformer. Recently, the conformational dependence of $Si_4(CH_3)_{10}$ on UV absorption has been investigated using singly excited configuration interaction (SE-CI) calculations.[19b] All-transoid is the most stable as well as $n = 6$. The excitation energies of $\sigma\sigma^*$ and $\sigma\pi^*$ are not dependent on conformational change, but oscillator strengths are strongly affected. More recently, the three conformers of n-$Si_4(CH_3)_{10}$ have been investigated using the complete active space−self consistent field method, and it has been shown that the excitation energies and ionization potentials are slightly affected by the conformational change. Also, the effects of conformations in the neutral state are clearly elucidated by their calculations. Thus, information on the electronic structures of neutral oligosilanes have been accumulated from theoretical points of view. On the other hand, few theoretical works have been carried out for radical ions of oligosilanes despite their importance.

In previous papers, we investigated the structures and electronic states of the polysilane radical anion[21] and cation[22] by means of the semiempirical third-parametric configuration interaction (PM3-CI) method. The permethyl oligosilane [$Si_n(Me)_{2n+2}$] ($n = 8-20$) with the all-trans form was chosen as a model of polysilane. We showed that excess electrons and holes are fully delocalized along the skeleton of linear polysilane if the structure has the regular all-trans form. The electronic excitation energy from the ground to first exited states was gradually red-shifted as a function of the number of chain Si atoms (n). Our previous studies suggested that the excess electron (hole) is not localized in the case of the regular all-trans form in the linear polysilane but is delocalized widely along the main chain. Also, the mechanism of electron localization at finite temperatures was investigated by means of MM2 molecular dynamics and PM3 methods.[23]

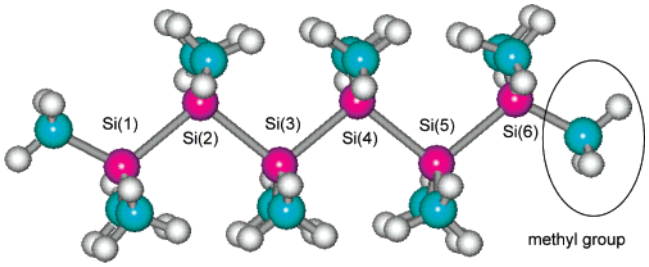

Figure 1. Schematic illustration of structure of permethyloligosilane, $Si_n(CH_3)_{2n+2}$ ($n = 6$), with all-trans form. Hydrogens in the methyl group are omitted from the figure.

More recently, Tada and Yoshimura have carried out SE-CI calculations for the radical anion of oligosilane Si_nH_{2n+2} ($n = 2-6$).[24] The ground state is composed of σ^* characteristics where an unpaired electron occupies the σ^* orbital of the Si−Si skeleton. The first electronic transition of $(Si_nH_{2n+2})^-$ ($n = 2-6$) is assigned to the Si−Si($\sigma^* \leftarrow \sigma^*$) transition. The π character appears from the third excited state. However, the radical anion $(Si_nH_{2n+2})^-$ has been not observed experimentally, and the conclusion may be therefore limited only to the $(Si_nH_{2n+2})^-$ system. Actual systems observed experimentally include alkyl groups (such as methyl and ethyl groups) in the side chain. Hence, studying of the electronic structures of methyl-substituted oligosilane is required to compare directly with the experiments.

In the present study, to interpret the experimental data obtained by Kumagai et al. from a theoretical point of view, density functional theory (DFT) calculations have been carried out for neutral permethyloligosilane and the radical cation and anion of permethyloligosilane with the all-trans form $Si_n(CH_3)_{2n+2}$ ($n = 2-6$). In particular, we focus our attention mainly on the assignment of the near-IR band and ESR spectra of the radical cation.

2. Method of Calculations

A linear oligosilane with methyl groups in the side chain, permethyl oligosilane [$Si_n(CH_3)_{2n+2}$; $n = 2-6$], was examined in the present work. The structure and atom numbers for $n = 6$ are illustrated in Figure 1. The structure of oligosilane for the neutral state was generated by direct PM3 molecular dynamics (MD) calculation[25] at 300 K. And then, the geometry was further optimized at the DFT(B3LYP)/6-311+G(d,p) level. The structures of the radical ions of oligosilane were fully optimized from the neutral structure at the B3LYP/6-311+G(d,p) level of theory. When the

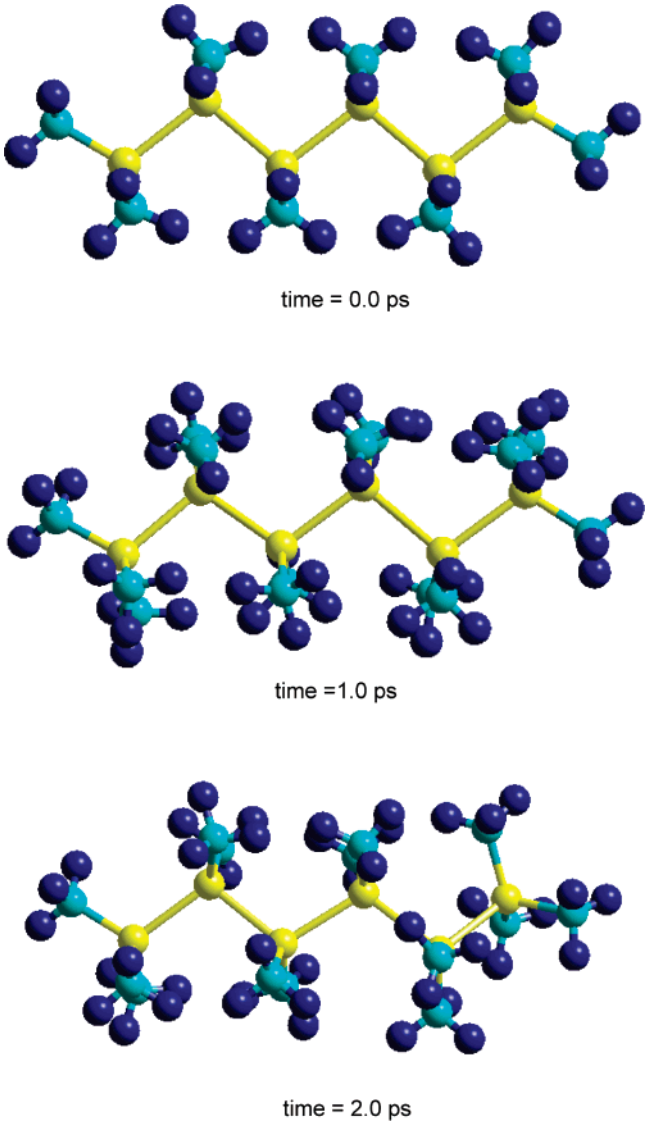

Figure 2. Snapshots of structural conformations of $Si_6(CH_3)_{14}$ obtained by direct PM3-MD calculation at 300 K.

optimized geometries were used, the excitation energies were calculated by means of time-dependent (TD)-DFT calculations at the B3LYP/6-311+G(d,p) level. Twelve excited states were solved in TD-DFT calculations. All hybrid DFT calculations were carried out using the Gaussian 03 program package.[26] Note that this level of theory gives reasonable features for several molecular device systems.[27−29]

3. Results

A. Structures of Permethyl Oligosilanes. First, the structure of oligosilane with the regular all-trans form is fully optimized by the semiempirical third-parametric molecular orbital (PM3-MO) method. Second, direct PM3 MD calculation[25] is carried out from the optimized structure to elucidate the effects of rotation of the methyl group (position of hydrogen atoms of the CH_3 group) on the structure and energetics. The mean temperature used in the MD calculation is 300 K. Results of the direct PM3-MD calculation for n = 6 are given in Figures2 and 3. The snapshots of oligosilane show that the structure of oligosilane is slightly deformed from the regular all-trans form by thermal activation. All

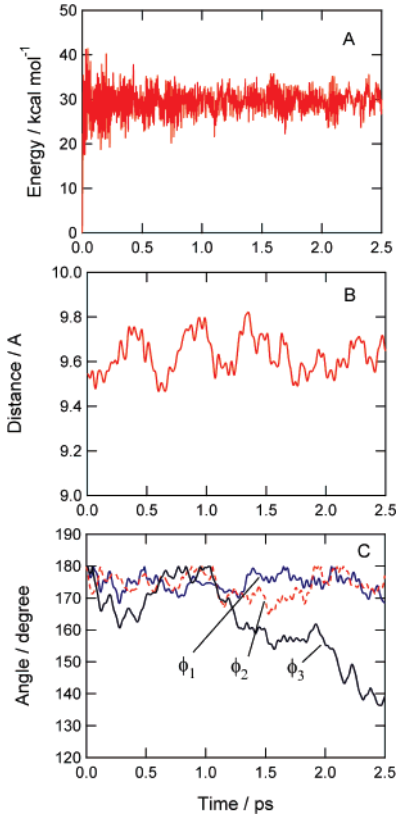

Figure 3. Results of direct PM3-MD calculation of $Si_6(CH_3)_{14}$ at 300 K. (A) Potential energy of the system, (B) the head-to-tail distance of the Si−Si main chain (in A), and (C) the dihedral angles.

dihedral angles are $\phi_1 = \phi_2 = \phi_3 = 180.0°$ at time zero, where the dihedral angles are defined as $\phi_1 = \angle$Si(1)−Si(2)−Si(3)−Si(4), $\phi_2 = \angle$Si(2)−Si(3)−Si(4)−Si(5), and $\phi_3 = \angle$Si(3)−Si(4)−Si(5)−Si(6). These angles are gradually changed as a function of time: $\phi_1 = 174.6°$, $\phi_2 = 177.3°$, and $\phi_3 = 179.5°$ at time = 1.0 ps and $\phi_1 = 174.0°$, $\phi_2 = 175.4°$, and $\phi_3 = 155.5°$ at 2.0 ps. However, the change of the main chain is not large. Instead, the rotation of hydrogen atoms of the methyl group is mainly enhanced by thermal activation.

Figure 3A−C show a potential energy of the system (n = 6), a distance between the head and tail silicon atoms in the main chain of oligosilane (defined by R), and the dihedral angles, respectively. The average of the potential energy becomes almost constant after time = 0.30 ps. The chain length (R) is gradually varied as a function of time (Figure 3B). However, the amplitude of R is only 0.32 Å, indicating that deformation of the main chain has hardly occurred at 300 K. The dihedral angles are plotted in Figure 3C. The angles are varied in the range 140−180°. However, large conformational changes, namely, rotation of the Si−Si bond, does not occur at 300 K. Only the rotation of the methyl group takes place at 300 K.

Next, a total number of 17 structures in the time range 1.0−2.5 ps are selected from the results of direct PM3-MD calculation, and then the geometries are fully optimized at the HF/3-21G(d) level. Initial and final energies of $Si_6(CH_3)_{14}$ before and after geometry optimization are summarized in Table 1. Relative energy is calculated on the basis of the

Table 1. Initial and Relaxed Energies before and after Geometry Optimization at Selected Points Obtained by Direct PM3-MD Calculation at 300 K[a]

selected point	time ps	initial total energy au	relaxed total energy au	initial energy[b] kcal/mol	final energy[b] kcal/mol
0	0.0	−2276.670 15	−2276.725 40	34.67	0.00
1	1.0	−2276.622 61	−2276.725 40	64.50	0.00
2	1.1	−2276.621 95	−2276.725 40	64.91	0.00
3	1.2	−2276.619 36	−2276.725 40	66.54	0.00
4	1.3	−2276.633 89	−2276.725 40	57.42	0.00
5	1.4	−2276.627 34	−2276.725 40	61.53	0.00
6	1.5	−2276.636 63	−2276.725 40	55.71	0.00
7	1.6	−2276.617 25	−2276.725 40	67.86	0.00
8	1.7	−2276.624 62	−2276.725 40	63.24	0.00
9	1.8	−2276.618 69	−2276.725 40	66.96	0.00
10	1.9	−2276.633 54	−2276.725 40	57.64	0.00
11	2.0	−2276.622 72	−2276.725 40	64.44	0.00
12	2.1	−2276.615 58	−2276.725 40	68.91	0.00
13	2.2	−2276.603 35	−2276.724 42	76.59	0.62
14	2.3	−2276.620 84	−2276.725 40	65.61	0.00
15	2.4	−2276.614 53	−2276.725 40	69.57	0.00
16	2.5	−2276.614 97	−2276.725 40	69.29	0.00

[a] The initial and relaxed total energies (in au) are calculated at the HF/3-21G(d) level. The geometry optimization is carried out at the HF/3-21G(d) level. [b] Zero-level corresponds to the energy level of the optimized structure at time zero.

total energy of the optimized geometry at time zero [HF/3-21G(d) level]. The initial energies are lying 35−77 kcal/mol above the zero level. After the geometry optimization, two energy minima are obtained. The geometry optimizations from the selected points give the same structure, except for one result for the selected point 13 in Table 1. This result indicated that thermal activation causes rotation of the methyl groups of the oligosilanes, but the positions of hydrogen atoms are a secondary matter. The geometry optimizations from these points give a unique structure with the all-trans form. The most stable structure is further optimized at the B3LYP/6-311+G(d,p) level.

The optimized parameters are given in Table 2. The position of the Si atom is defined in Figure 1. The geometry optimization gives no-symmetry structures for all oligosilanes ($n = 2-6$). The Si skeleton of the oligomer is not in plane, and the dihedral angles of Si−Si−Si−Si are close to 160° at the B3LYP/6-311+G(d,p) level. The Si−Si bond length is close to 3.8 Å for all neutral oligosilanes. For example, the bond lengths for $n = 3$ are calculated to be 2.3790 Å, which is significantly close to the previous theoretical value (2.3533 Å at the MP2/cc-pVTZ level)[30] and the experimental value (2.325 Å).[31]

For the radical cation, the Si−Si bond lengths are longer than those of the neutral state. This elongation is due to the fact that an electron is removed from a Si−Si σ bond of the oligomer. The structures of radical anions are also fully optimized at the same level of theory. The structures for $n = 2-4$ are hardly changed by accepting an excess electron. On the other hand, the bond lengths of $n = 5$ and 6 are largely elongated. For example, a Si−Si bond in the central position for $n = 6$, Si(3)−Si(4), is elongated from 2.3887 to 2.4426 Å.

Band gaps of neutral oligosilanes ($n = 2-6$), estimated by the energy difference between the highest occupied molecular orbital (HOMO) and lowest unoccupied molecular orbital (LUMO), decrease gradually from 6.42 to 5.38 eV as chain lengths are increased from $n = 2$ to 6. The adiabatic ionization potential (without zero-point energy, ZPE) decreases gradually with increasing n: 7.80 eV ($n = 2$) and 6.78 eV ($n = 6$). Adiabatic electron affinities (without ZPE) are varied from −0.58 eV ($n = 2$) to −0.15 eV ($n = 6$).

B. Excitation Energies of Neutral Oligosilanes ($n = 2-6$). The low-lying excited state correlates strongly with the electron conductivity in organic semiconductors. Hence, the electronic structures for the excited states are determined in this system. The excitation energies calculated for the neutral oligosilanes with the transoid form are given in Table 3. The first electronic transition for $n = 2$ occurs at 6.15 eV with an oscillator strength $f = 0.053$. A stronger electronic transition appears at 6.30 eV with $f = 0.123$. The first electronic excitation band with the large oscillator strength is gradually red-shifted with increasing chain length (n): for example, the excitation energies are 5.38 eV ($n = 3$), 5.30 eV ($n = 4$), 4.98 eV ($n = 5$), and 4.77 eV ($n = 6$). It is also shown that the first electronic transitions are nearly degenerated in $n = 3-6$. The absorption band is assigned to the HOMO(σ) → LUMO(σ^*) transition for $n = 3-6$, but that for $n = 2$ is a $\sigma-\pi^*$ transition. For $n = 2$, the lowest excited state is calculated to be 5.73 eV ($f = 0.0$), which is assigned to a Rydberg state. This is caused by underestimation of the excitation energy due to a diffuse orbital on the hydrogen atoms. The assignment of the excitation essentially agrees with previous theoretical work by Rooklin et al.[32]

To check the reliability of the level of theory used in the present calculation, the excitation energies are compared with the experiments. The results are given in Table 4. The experimental excitation energies measured at 77 K in 2-methyltetrahydrofuran matrixes for $n = 4$, 5, and 6 are 5.28, 4.96, and 4.77 eV, respectively. The corresponding

Table 2. Optimized Geometrical Parameters for Neutral Molecule and the Radical Cation and Radical Anion of Oligosilanes (Transoid) Calculated at the B3LYP/6-311+G(d,p) Level

		Bond Length				
state	*n*	$R(Si^1-Si^2)$	$R(Si^2-Si^3)$	$R(Si^3-Si^4)$	$R(Si^4-Si^5)$	$R(Si^5-Si^6)$
neutral	2	2.3741				
	3	2.3790	2.3790			
	4	2.3801	2.3803	2.3801		
	5	2.3787	2.3853	2.3853	2.3787	
	6	2.3821	2.3862	2.3887	2.3862	2.3821
cation	2	2.7103				
	3	2.5022	2.5022			
	4	2.4772	2.4273	2.4772		
	5	2.4434	2.4343	2.4343	2.4434	
	6	2.4288	2.4269	2.4409	2.4269	2.4287
anion	2	2.3680				
	3	2.3796	2.3796			
	4	2.3789	2.3832	2.3789		
	5	2.3991	2.4458	2.4458	2.3991	
	6	2.3917	2.4217	2.4426	2.4217	2.3917

		Dihedral Angle		
state	*n*	ϕ_1	ϕ_2	ϕ_3
neutral	4	165.2		
	5	165.0	165.0	
	6	168.2	171.5	168.2
cation	4	165.2		
	5	163.9	163.9	
	6	165.1	163.3	165.1
anion	4	180.0		
	5	180.0	180.0	
	6	180.0	180.0	172.6

Table 3. Excitation Energies (in eV) and Oscillator Strengths (Given in Parentheses) of Neutral Oligosilanes with Transoid Form ($n = 2-6$) Calculated at the B3LYP/6-311+G(d,p) Level

state	$n = 2$	3	4	5	6
1^{st}	5.73 (0.0000)σR[a]	5.38 (0.0373)$\sigma\sigma^*$	5.20 (0.0005)$\sigma\pi^*$	4.98 (0.2750)$\sigma\sigma^*$	4.77 (0.6173)$\sigma\sigma^*$
2^{nd}	6.15 (0.0529)$\sigma\pi^*$	5.57 (0.0000)$\sigma\pi^*$	5.22 (0.0039)$\sigma\pi^*$	4.99 (0.000)σR	4.87 (0.0009)$\sigma\pi^*$
3^{rd}	6.15 (0.0529)$\pi\pi^*$	5.75 (0.0134)$\sigma\sigma^*$	5.30 (0.1977)$\sigma\sigma^*$	5.10 (0.0729)$\sigma\pi^*$	4.96 (0.0002)σR
4^{th}	6.30 (0.1226)$\sigma\sigma^*$	5.92 (0.0057)$\sigma\sigma^*$	5.58 (0.0523)$\sigma\sigma^*$	5.34 (0.0054)$\sigma\pi^*$	5.20 (0.0201)$\sigma\pi^*$
Rooklin[b]	6.76	5.95	5.48	5.23	4.96
Obtara[c]	6.44	5.73	5.28	4.96	4.77

[a] σ-Rydberg transition. [b] Theoretical value by Rooklin et al. cited from ref 32. [c] Experimental value by Obara and Kira cited from ref 33.

calculated excitation energies are 5.30 ($n = 4$), 4.98 ($n = 5$), and 4.77 eV ($n = 6$). The excitation energies measured in an argon matrix at 10 K are 6.63 ($n = 2$) and 5.93 eV ($n = 3$), which are also in reasonable agreement with the present calculations, 6.15 ($n = 2$) and 5.38 eV ($n = 3$), although the calculation underestimates slightly the excitation energies for shorter oligomers. The agreement with the experiments indicates that the TD-DFT(B3LYP)/6-311+G(d,p) calculation gives reasonable electronic transition energy for the oligosilane system.

C. Electronic States of Radical Cations. 1. Spin Density and g Value. Spin densities on protons of the methyl groups in the radical cation are given in Table 5. The value is averaged on each Si segment $-Si(m)(CH_3)_2-$ (where $m = 1-6$). For $n = 6$, spin densities on segment Si(m) where $m = 1-6$ are 0.138, 0.148, 0.214, 0.214, 0.148, and 0.138, respectively, indicating that an unpaired electron (or hole) is delocalized on the Si skeleton.

In general, ESR spectra of the radical cation of oligosilane show a broad single band without a hyperfine structure except for $n = 2$. Only the radical cation for $n = 2$ has a spectrum with a hyperfine structure. The hyperfine coupling constant of the hydrogen atom (H-hfcc) for $n = 2$ has been measured directly to be 0.57 mT.[18] The H-hfcc for $n = 2$ is calculated to be 0.552 mT in the present study, which is in good agreement with the ESR experiment. For $n = 4-6$, there is

Table 4. Comparison of Theoretical and Experimental Excitation Energies (E_{ex} in eV) and Wavelengths (λ_{max} in nm) at Maximum Peak Positions of Neutral Oligosilanes $Si_n(CH_3)_{2n+2}$ ($n = 2-6$)

	theoretical		experimental[a]	
n	λ_{max}	E_{ex}	λ_{max}	E_{ex}
2	202	6.15	187	6.63[a]
3	230	5.38	209	5.93[a]
4	234	5.30	235	5.28[b]
(4a,4g)[c]				(5.44,5.96)[a]
5	249	4.98	250	4.96[b]
(5aa,5ga,5gg)[c]				(5.05,5.39,5.94)[a]
6	260	4.77	260	4.77[b]

[a] In argon matrix at 10 K cited from ref 19. [b] In 2-methyltetrahydrofuran (MTHF) at 77 K cited from ref 16. [c] Notations "a" and "g" mean "anti" and "gauche", respectively.

Table 5. Proton-Hyperfine Coupling Constants (H-hfcc's) of the Radical Cation of Oligosilane (in mT) and Spin Densities on Each Subsegment of $Si(m)(Me)_2$ ($m = 1-6$) Calculated at the B3LYP/6-311+G(d,p) Level

n	state	Si(1)	Si(2)	Si(3)	Si(4)	Si(5)	Si(6)
2	hfcc	0.552	0.552				
	spin	0.50	0.50				
3	hfcc	0.362	0.531	0.362			
	spin	0.336	0.329	0.336			
4	hfcc	0.259	0.339	0.339	0.259		
	spin	0.241	0.259	0.259	0.241		
5	hfcc	0.186	0.262	0.278	0.262	0.186	
	spin	0.181	0.186	0.266	0.186	0.181	
6	hfcc	0.137	0.197	0.243	0.243	0.197	0.137
	spin	0.138	0.148	0.214	0.214	0.148	0.138

Table 6. **g**-Tensor Components of the Radical Cation of Oligosilanes Calculated at the B3LYP/6-311+G(d,p) Level

n	g_{xx}	g_{yy}	g_{zz}
2	2.0023	2.0102	2.0102
3	2.0033	2.0095	2.0173
4	2.0029	2.0094	2.0184
5	2.0028	2.0095	2.0191
6	2.0027	2.0097	2.0191

no direct experimental value because of its broad single spectrum, while simulated hfcc's were estimated: for example, H-hfcc's for $n = 6$ are estimated to be 0.11, 0.29, and 0.39 mT from the simulation. The calculated values are 0.137, 0.197, and 0.243 mT, which are in reasonable agreement with the simulated values.

Isosurfaces of spin densities for $n = 3-6$ are illustrated in Figure 4. It is shown that the spin−orbital is composed of a σ(Si−Si) orbital and an unpaired electron that is widely distributed over the oligomer.

A **g**-tensor component gives important information on the electronic structure of the paramagnetic compound at the ground state. The values of oligosilanes ($R = CH_3$) calculated at the B3LYP/6-311+G(d,p) level are given in Table 6. It is found that the anisotropy of the **g**-value for the radical cation of oligosilane is significantly small, and those are close to that of the free electron ($g_e = 2.0023$). For $n = 2$, the

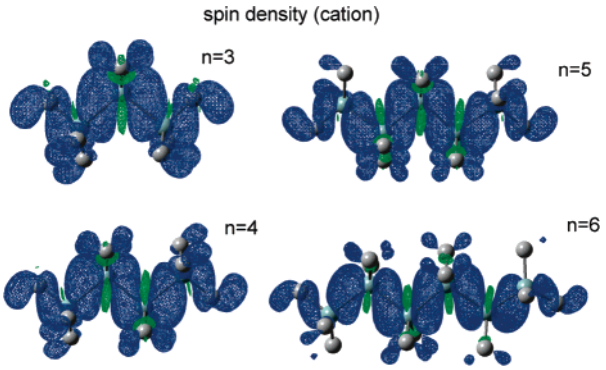

Figure 4. Illustrations of spin densities of radical cations of oligosilanes ($n = 3-6$) at the ground state.

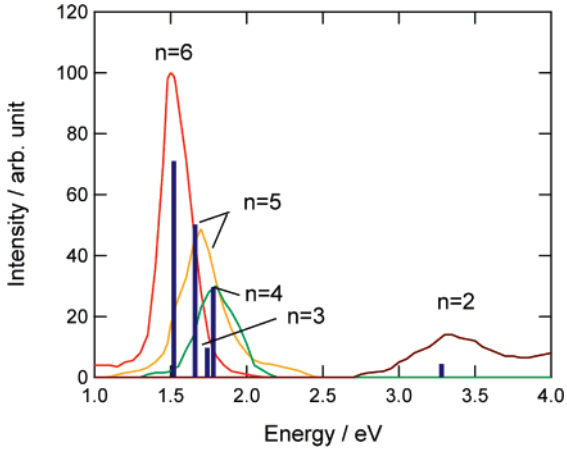

Figure 5. Calculated (stick diagram) and experimental absorption spectra (solid curve) of radical cations of oligosilane ($n = 3-6$). Experimental data are cited from ref 18.

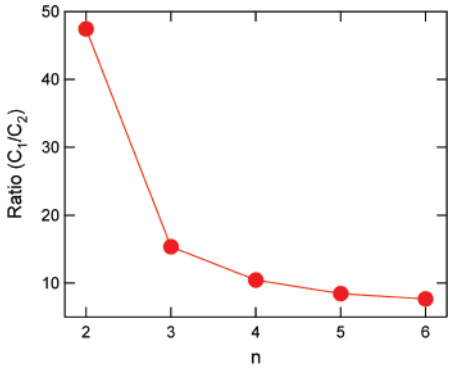

Figure 6. Ratio of coefficients (C_1/C_2) of reference functions (C_1 and C_2) as a function of *n*.

averaged *g* value is $\langle g \rangle = 2.0076$, which is in good agreement with the experimental value [$\langle g \rangle = 2.008$ measured for $Si_2(CH_3)_6^+$ at 77 K].[18] The calculation shows that the averaged *g* value increases slightly with increasing *n*, but the magnitude of the increase is small: $\langle g \rangle = 2.0076$ ($n = 2$), 2.0100 ($n = 3$), 2.0102 ($n = 4$), 2.0105 ($n = 5$), and 2.0105 ($n = 6$). These values agree well with those of the popular radical cations of poly- and oligosilanes: for example, radical cations of poly(cyclohexylmethylsilane) and poly(methylphenylsilane) have $\langle g \rangle = 2.008$, which is larger than that of the free electron (g_e).[18]

Table 7. Excitation Energies (in eV) and Oscillator Strengths (Given in Parentheses) of the Radical Cation of Oligosilanes, $[Si_n(CH_3)_{2n+2}]^+$ ($n = 2-6$), Calculated at B3LYP/6-311+G(d,p) Level[a]

state	$n = 2$	3	4	5	6
1st	3.05 (0.0000)	*1.74 (0.0524)*	*1.78 (0.1647)*	*1.66 (0.2788)*	*1.52 (0.3944)*
2nd	3.06 (0.0000)	2.75 (0.0005)	2.08 (0.0006)	2.08 (0.0001)	2.03 (0.0005)
3rd	*3.28 (0.0124)*	2.89 (0.0018)	2.86 (0.0033)	2.19 (0.0127)	2.20 (0.0084)
4th	*3.28 (0.0124)*	2.89 (0.0130)	2.88 (0.0025)	2.86 (0.0068)	2.27 (0.0004)
5th	5.07 (0.0000)	2.97 (0.0389)	2.94 (0.0451)	2.87 (0.0002)	2.86 (0.0017)
6th	5.24 (0.0000)	3.16 (0.0000)	3.00 (0.0000)	2.96 (0.0263)	2.86 (0.0023)

[a] Italic characters mean the first excitation energies with a nonzero oscillator strength.

Table 8. Proton-Hyperfine Coupling Constants (hfcc's) of the Radical Anion of Oligosilane (in mT) and Spin Densities on Each Subsegment of Si(m)(Me)$_2$ ($m = 1-6$) Calculated at the B3LYP/6-311+G(d,p) Level

n	state	Si(1)	Si(2)	Si(3)	Si(4)	Si(5)	Si(6)
2	hfcc	0.044	0.044				
	spin	0.500	0.500				
3	hfcc	0.030	0.036	0.030			
	spin	1.115	−1.229	1.115			
4	hfcc	0.027	0.026	0.026	0.027		
	spin	0.739	−0.240	−0.239	0.739		
5	hfcc	0.064	0.043	0.046	0.043	0.064	
	spin	0.187	0.206	0.213	0.206	0.187	
6	hfcc	0.049	0.031	0.041	0.041	0.031	0.049
	spin	0.141	0.155	0.204	0.204	0.155	0.141

Table 9. **g**-Tensor Components of the Radical Anion of Oligosilanes Calculated at the B3LYP/6-311+G(d,p) Level[a]

		g_{xx}	g_{yy}	g_{zz}
calcd (R = −H)	2	2.0019	2.0032	2.0051
	3	2.0021	2.0031	2.0059
	4	2.0019	2.0031	2.0068
	5	2.0019	2.0031	2.0075
	6	2.0018	2.0031	2.0081
calcd (R = $-CH_3$)	2	2.0025	2.0027	2.0027
	3	2.0026	2.0027	2.0027
	4	2.0006	2.0020	2.0063
	5	2.0006	2.0020	2.0064
	6	2.0002	2.0021	2.0064
exptl (R = $-CH_3$)[a]	4	1.9979	2.0037	2.0082
	5	1.9992	2.0032	2.0061
	6[b]	2.0032	2.0032	2.0032

[a] Experimental **g** tensors are cited from ref 17. [b] Experimental values are $g_{xx} \approx g_{yy} \approx g_{zz}$.

C.2. Excitation Energy. Figure 5 shows the first excitation energies and its oscillator strengths calculated for the radical cation of $Si_n(CH_3)_{2n+2}$ ($n = 2-6$) together with experimental absorption spectra measured by Kumagai et al.[18] Unfortunately, the absorption spectrum for $n = 3$ has not been observed yet. Hence, the experimental spectra for $n = 2$ and 4−6 are depicted in the figure. The present calculation represents excellently the absorption spectra derived from the experiment. This agreement implies that the level of theory is adequate enough to discuss the electronic states of the radical cation.

The low-lying excitation energies calculated for the radical cation are given in Table 7. The first electronic transition for $n = 2$ is calculated to lie at 3.28 eV with an oscillator strength $f = 0.0124$. The excitation energy becomes significantly lower in the case of a longer oligosilane, $n = 3$ (1.74 eV), and also the oscillator strength becomes larger ($f = 0.0524$) in $n = 3$. The excitation energy and oscillator strength for $n = 6$ are 1.522 eV and $f = 0.3944$, respectively. In larger oligomers, the excitation energy is gradually red-shifted and the oscillator strength increases with increasing n.

We found that the first excited state with a nonzero oscillator strength for the radical cation (electronic transition corresponds to the near-IR band) is composed of two electronic states, ψ_1(HOMO → SOMO) and ψ_2(SOMO → SOMO + m), where HOMO and SOMO mean the highest doubly occupied and singly occupied molecular orbitals of the radical cation, respectively, and m means an integer. The first excited state is expressed by

$$\Psi\,(1\mathrm{st}) = C_1\psi_1(\mathrm{HOMO} \rightarrow \mathrm{SOMO}) + C_2\psi_2(\mathrm{SOMO} \rightarrow \mathrm{LUMO}) + \ldots.$$

For $n = 2$, the coefficients C_1 and C_2 are calculated to be 0.997 and −0.021, respectively, indicating that the main configuration is ψ_1(HOMO → SOMO) at the first excited state. For $n = 6$, the coefficients are significantly changed to $C_1 = 0.901$ and $C_2 = -0.118$. Figure 6 shows absolute values of the ratio of C_1 and C_2 plotted as a function of n. The ratio reaches a limited value in larger n values. For $n = 6$, the weight of ψ_1(HOMO → SOMO) is calculated to be 0.81. This result means that the near-IR band in poly- and oligosilanes is assigned to an electronic transition ψ_0(SOMO) → ψ_1(HOMO → SOMO). Also, it can be expected that the UV band appearing at 250−350 nm is caused by electronic transitions from SOMO → LUMO and HOMO → LUMO + m. It can be concluded that the strong band of the radical cation is assigned to the valence transition within the Si−Si σ bond.

D. Electronic States of Radical Anions. 1. Spin Density and g Value. Spin densities of radical anions of oligosilanes calculated are given in Table 8, and isosurfaces of spin densities for $n = 5$ and 6 are illustrated in Figure 7. The unpaired electron is delocalized over the Si skeleton of oligosilane, while electron localization is not found in the range $n = 2-6$. For example, the spin densities on the Si subunits for $SiMe_3$(1), $SiMe_2$(2), $SiMe_2$(3), $SiMe_2$(4), $SiMe_2$-(5), and $SiMe_3$(6) are calculated to be 0.141, 0.155, 0.204, 0.204, 0.155, and 0.141, respectively. H-hfcc's for $n = 6$ are distributed in the rage 0.031−0.049 mT, which are significantly smaller than those of the radical cation. This is due to the fact that the unpaired electron is located on a σ*-

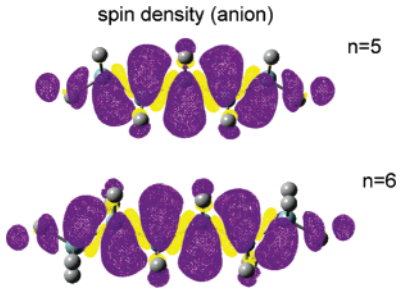

Figure 7. Illustrations of spin densities of radical anions of oligosilanes ($n = 5$ and 6) at the ground state.

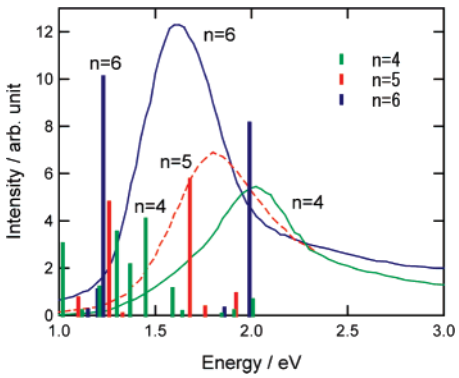

Figure 8. Calculated (stick diagram) and experimental absorption spectra (solid curve) of the radical anions of oligosilane ($n = 4-6$).

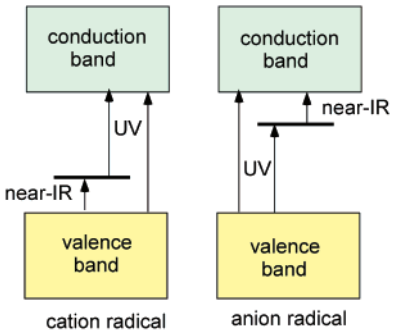

Figure 9. Schematic illustration of band structures of radical ions of oligosilanes.

(Si−Si) orbital mixed with a diffuse-type orbital in the radical anion, so that spin density in the 1s orbital of the proton is significantly diminished.

The **g**-tensor components of radical anions of oligosilanes (R = −H and $-CH_3$) are given in Table 9. The calculation shows that the component g_{xx} is slightly lower than that of the free electron ($g_e = 2.0023$), whereas g_{zz} is larger than g_e. On the other hand, g_{yy} is close to g_e. These features are in reasonable agreement with experimental values: for example, the g values for $n = 5$ are measured to be $g_{xx} = 1.9992$ ($< g_e$), $g_{yy} = 2.0032$ ($= g_e$), and $g_{zz} = 2.0061$ ($> g_e$). For R = −H and $-CH_3$, similar spectral features are obtained.

D.2. Excitation Energy. The low-lying excitation energies for the radical anion of oligosilane are given in Table 10. The first electronic transition for $n = 6$ is calculated in the range 0.69−1.20 eV with an oscillator strength $f = 0.0038-0.0803$. From the TD-DFT calculation, it is found that the near-IR band is assigned to the (HOMO − m) → SOMO (where $m = 0-10$) transition. The strong band of the radical anion is assigned to the valence transition within the Si−Si σ bond. Figure 8 shows the excitation energies and its oscillator strengths calculated for the radical anion of $Si_n(CH_3)_{2n+2}$ ($n = 4-6$) together with experimental absorption spectra. It seems that there is disagreement between theory and experiment in the radical anion: the excitation energies calculated are underestimated in all cases. This discrepancy may be caused by the contribution of two- and three-electron excitations to the excited-state wave function.

4. Discussion

A. Summary of the Present Study. In the present study, hybrid DFT calculations have been carried out for the neutral and radical ions of oligosilane, $Si_n(CH_3)_{2n+2}$ ($n = 2-6$), to elucidate the electronic structures of radical ions of oligosilane. In both radical ions, holes and excess electrons are delocalized along the Si chain at the ground state. These characteristics are in good agreement with previous theoretical[21−24] and experimental characteristics.[13,14,16−18]

For the radical cation, the unpaired electron (hole) is occupied in the σ(Si−Si) orbital, whereas the excess electron in the radical anion is occupied in the σ^*(Si−Si) orbital mixing slightly with a π state of the Si−C bond and a diffuselike orbital. The magnetic properties obtained by the present calculations, g values and hyperfine hfcc's, are in good agreement with experiments.[17,18]

The first excited state for the radical cation is composed mainly of the ψ(HOMO → SOMO) state (weight of reference is about 0.80), and the ψ(SOMO → LUMO) state is contributed to the first excited state. The calculations indicate that this state appears as a near-IR band. Also, the other low-lying excited sites of the radical cation consist of ψ(HOMO − m → SOMO) states (where m means an integer), but the excitation to these states has a small oscillator strength. It is also expected that the UV band

Table 10. Excitation Energies (in eV) and Oscillator Strengths (Given in Parentheses) of the Radical Anion of Oligosilanes, $[Si_n(CH_3)_{2n+2}]^-$ ($n = 2-6$), Calculated at the B3LYP/6-311+G(d,p) Level

state	$n = 2$	3	4	5	6
1st	0.49 (0.1630)	0.40 (0.1186)	0.30 (0.0811)	0.71 (0.0027)	0.69 (0.0803)
2nd	0.49 (0.1626)	0.47 (0.1716)	0.32 (0.1353)	0.75 (0.0994)	0.76 (0.0000)
3rd	0.54 (0.2831)	0.51 (0.2928)	0.39 (0.2084)	0.85 (0.0036)	0.86 (0.0000)
4th	1.18 (0.0000)	0.87 (0.0242)	0.72 (0.0001)	1.10 (0.0128)	1.11 (0.0011)
5th	1.18 (0.0000)	0.92 (0.0095)	0.75 (0.0010)	1.23 (0.0000)	1.15 (0.0038)
6th	1.34 (0.0000)	1.00 (0.0033)	0.79 (0.0010)	1.26 (0.0838)	1.20 (0.0188)

appearing at 250−350 nm is caused by electronic transitions from SOMO to LUMO and HOMO to LUMO + *m*.

B. Band Structure of Radical Ions of Oligosilanes. From the characteristics of the coefficients (C_1 and C_2) and the ratio (C_1/C_2), it is found that concept of the electronic states of the radical anion of oligosilane can be expanded to longer oligosilanes and polysilanes. On the basis of the present calculations, the band structures for radical ions of longer oligosilanes are expected and illustrated schematically in Figure 9. The horizontal lines drawn between valence and conduction bands mean cation (left) and anion (right) states of oligo- and polysilanes. The energy level of the cation state of oligosilane is slightly higher than the valence band because the SOMO of the cation state is mainly originated from the HOMO of neutral oligosilane. From the present calculation, it is expected that the near-IR band is assigned to the electronic transition from the valence band to the cation state, although the electronic transition from the cation state to the conduction band is slightly contaminated to the near-IR band. The UV band is attributed to the electronic transition from the valence band to the conduction band, which is energetically perturbed by the cation state.

The band structure of the radical anion of oligo- and polysilanes is also illustrated. The energy level of the anion state is lower than the bottom of the conduction band. The present calculation predicts that electronic transition from the anion state to the valence band is observed as a near-IR band. The UV band is assigned to the excitation from the valence to the anion state and that from the valence to the conduction bands.

C. Remarks. In the present study, DFT and TD-DFT (B3LYP) methods are applied to the neutral molecule and radical ions of oligosilane, $Si_n(CH_3)_{2n+2}$ ($n = 2-6$). The electronic structures, hfcc's, *g* values, and excitation energies for the neutral molecule and radical cation of oligosilanes were in good agreement with the experiments. However, this level of theory gave a poor result for excitation energies of the radical anion. To obtain a reasonable absorption spectrum of the radical anion, a more accurate wave function would be required. Despite the several assumptions introduced here, the results enable us to obtain valuable information on the electronic states of radical ions of oligosilanes.

Acknowledgment. The authors are indebted to the Computer Center at the Institute for Molecular Science (IMS) for the use of the computing facilities. Also, the authors acknowledge partial support from the president's optional budget from Kyoto University. One of the authors (H.T.) acknowledges a partial support from a Grant-in-Aid for Scientific Research (C) from the Japan Society for the Promotion of Science (JSPS).

References

(1) Miller, R. D.; Michl, J. *Chem. Rev.* **1989**, *89*, 1359.

(2) Kepler, R. G.; Zeigler, J. M.; Harrah, L. A.; Kurtz, S. R. *Phys. Rev. B: Condens. Matter Mater. Phys.* **1987**, *35*, 2818.

(3) Suzuki, H.; Meyer, H.; Hoshino, S. *J. Appl. Phys.* **1995**, *78*, 2684.

(4) Hoshino, S.; Suzuki, H. *Appl. Phys. Lett.* **1996**, *69*, 224.

(5) Fujii, A.; Yoshimoto, K.; Yoshida, M.; Ohmori, Y.; Yoshino, K. *Jpn. J. Appl. Phys.* **1995**, *34*, L1365.

(6) Hattori, R.; Sugano, T.; Shirafuji, J.; Fujiki, T. *Jpn. J. Appl. Phys.* **1996**, *35*, L1509.

(7) Suzuki, H.; Hoshino, S.; Yuan, C. H.; Fujiki, M.; Toyoda, S.; Matsumoto, N. *IEEE J. Quantum Electron.* **1998**, *4* (1), 129.

(8) Suzuki, H.; Hoshino, S.; Yuan, C. H.; Fujiki, M.; Toyoda, S.; Matsumoto, N. *Thin Solid Films* **1998**, *331*, 64.

(9) Xu, Y.; Fujino, T.; Watase, S.; Naito, H.; Oka, K.; Dohmaru, T. *Jpn. J. Appl. Phys.* **1999**, *38*, 2609.

(10) Suzuki, H.; Hoshino, S.; Furukawa, K.; Ebata, K.; Yuan, C. H.; Bleyl, I. *Polym. Adv. Technol.* **2000**, *11*, 460.

(11) Ban, H.; Sukegawa, K.; Tagawa, S. *Macromolecules* **1987**, *20*, 1775.

(12) Ban, H.; Sukegawa, K.; Tagawa, S. *Macromolecules* **1988**, *21*, 45.

(13) Irie, S.; Oka, K.; Irie, M. *Macromolecules* **1988**, *21*, 110.

(14) Irie, S.; Irie, M. *Macromolecules* **1992**, *25*, 1766.

(15) Ushida, K.; Kira, A.; Tagawa, S.; Yoshida, Y.; Shibata, H. *Polym. Prepr. (Am. Chem. Soc., Div. Polym. Mater.)* **1992**, *66*, 299.

(16) Irie, S.; Irie, M. *Macromolecules* **1997**, *30*, 7906.

(17) Kumagai, J.; Yoshida, H.; Koizumi, H.; Ichikawa, T. *J. Phys. Chem.* **1994**, *98*, 13117.

(18) Kumagai, J.; Yoshida, H.; Ichikawa, T. *J. Phys. Chem.* **1995**, *99*, 7965.

(19) (a) Ottosson C. H.; Michl, J. *J. Phys. Chem. A* **2000**, *104*, 3367. (b) Tsuji, T.; Michl, J.; Tamao, K. *J. Organomet. Chem.* **2003**, *685*, 9. (c) Plitt, H. S.; Downing, J. W.; Raymond, M. K.; Balaji, V.; Michl, J. *J. Chem. Soc. Faraday Trans.* **1994**, *90*, 1653. (d) Piqueras, M. C.; Crespo, R.; Michl, J. *J. Phys. Chem. A* **2003**, *107*, 4661.

(20) Sharma, A.; Lourderaj, U.; Deepak; Sathyamurthy, N. *J. Phys. Chem. B* **2005**, *109*, 15860.

(21) Tachikawa, H. *Chem. Phys. Lett.* **1997**, *281*, 221.

(22) Tachikawa, H. *Chem. Phys. Lett.* **1997**, *265*, 455

(23) Tachikawa, H. *J. Phys. Chem. A* **1999**, *103*, 2501.

(24) Tada, T.; Yoshimura, R. *J. Phys. Chem. A* **2003**, *107*, 6091.

(25) Tachikawa, H.; Shimizu, A. *J. Phys. Chem. B* **2005**, *109*, 13255.

(26) Frisch, M. J.; Trucks, G. W.; Schlegel, H. B.; Scuseria, G. E.; Robb, M. A.; Cheeseman, J. R.; Montgomery, J. A., Jr.; Vreven, T.; Kudin, K. N.; Burant, J. C.; Millam, J. M.; Iyengar, S. S.; Tomasi, J.; Barone, V.; Mennucci, B.; Cossi, M.; Scalmani, G.; Rega, N.; Petersson, G. A.; Nakatsuji, H.; Hada, M.; Ehara, M.; Toyota, K.; Fukuda, R.; Hasegawa, J.; Ishida, M.; Nakajima, T.; Honda, Y.; Kitao, O.; Nakai, H.; Klene, M.; Li, X.; Knox, J. E.; Hratchian, H. P.; Cross, J. B.; Bakken, V.; Adamo, C.; Jaramillo, J.; Gomperts, R.; Stratmann, R. E.; Yazyev, O.; Austin, A. J.; Cammi, R.; Pomelli, C.; Ochterski, J. W.; Ayala, P. Y.; Morokuma, K.; Voth, G. A.; Salvador, P.; Dannenberg, J. J.; Zakrzewski, V. G.; Dapprich, S.; Daniels, A. D.; Strain, M. C.; Farkas, O.; Malick, D. K.; Rabuck, A. D.; Raghavachari, K.; Foresman, J. B.; Ortiz, J. V.; Cui, Q.; Baboul, A. G.; Clifford, S.; Cioslowski, J.; Stefanov, B. B.; Liu, G.; Liashenko, A.; Piskorz, P.; Komaromi, I.; Martin, R. L.; Fox, D. J.; Keith,

T.; Al-Laham, M. A.; Peng, C. Y.; Nanayakkara, A.; Challacombe, M.; Gill, P. M. W.; Johnson, B.; Chen, W.; Wong, M. W.; Gonzalez, C.; Pople, J. A. *Gaussian 03*, revision B.04; Gaussian, Inc.: Wallingford, CT, 2004.

(27) Tachikawa, H.; Kawabata, H. *J. Mater. Chem.* **2003**, *13*, 1293

(28) Tachikawa, H.; Kawabata, H. *J. Phys. Chem. B* **2003**, *107*, 1113.

(29) Tachikawa, H.; Kawabata, H. *J. Phys. Chem. B* **2005**, *109*, 3139.

(30) Piqueras, M. C.; Crespo, R. *Mol. Phys.* **2006**, *104*, 1107.

(31) Almenningen, A.; Fjeldberg, T.; Eclwin, H. *J. Mol. Struct.* **1984**, *112*, 239.

(32) Rooklin, D. W.; Schepers, T.; Raymond-Johansson, M. K.; Michl, J. *Photochem. Photobiol. Sci*. **2003**, *2*, 511.

(33) Obata, K.; Kira, M. *Organometallics* **1999**, *18*, 2216.

CT600163R